Machine learning endometrial cancer risk prediction model: integrating guidelines of European Society for Medical Oncology with the tumor immune framework

Valentina Bruno,[1] Martina Betti ,[2] Lorenzo D'Ambrosio ,[3] Alice Massacci,[3] Benito Chiofalo,[1] Adalgisa Pietropolli,[4] Giulia Piaggio,[3] Gennaro Ciliberto,[3] Paola Nisticò,[3] Matteo Pallocca,[3] Alessandro Buda ,[5] Enrico Vizza[1]

OPEN ACCESS

► Additional supplemental material is published online only. To view, please visit the journal online (http://dx.doi.org/10.1136/ijgc-2023-004671).

For numbered affiliations see end of article.

Correspondence to
Dr Valentina Bruno, Department of Experimental Clinical Oncology, IRCCS Regina Elena National Cancer Institute, Rome 00144, Italy; valentina.bruno@ifo.it

VB, MB and LD'A contributed equally.
MP, AB and EV contributed equally.

Received 25 May 2023
Accepted 31 August 2023
Published Online First 24 October 2023

ABSTRACT

Objective Current prognostic factors for endometrial cancer are not sufficient to predict recurrence in early stages. Treatment choices are based on the prognostic factors included in the risk classes defined by the ESMO-ESGO-ESTRO (European Society for Medical Oncology-European Society of Gynaecological Oncology-European Society for Radiotherapy and Oncology) consensus conference with the new biomolecular classification based on POLE, TP53, and microsatellite instability status. However, a minority of early stage cases relapse regardless of their low risk profiles. Integration of the immune context status to existing molecular based models has not been fully evaluated. This study aims to investigate whether the integration of the immune landscape in the tumor microenvironment could improve clinical risk prediction models and allow better profiling of early stages.

Methods Leveraging the potential of in silico deconvolution tools, we estimated the relative abundances of immune populations in public data and then applied feature selection methods to generate a machine learning based model for disease free survival probability prediction.

Results We included information on International Federation of Gynecology and Obstetrics (FIGO) stage, tumor mutational burden, microsatellite instability, POLEmut status, interferon γ signature, and relative abundances of monocytes, natural killer cells, and CD4+T cells to build a relapse prediction model and obtained a balanced accuracy of 69%. We further identified two novel early stage profiles that undergo different pathways of recurrence.

Conclusion This study presents an extension of current prognostic factors for endometrial cancer by exploiting machine learning models and deconvolution techniques on available public biomolecular data. Prospective clinical trials are advisable to validate the early stage stratification.

WHAT IS ALREADY KNOWN ON THIS TOPIC

⇒ Prognostic factors defined by the ESMO-ESGO-ESTRO (European Society for Medical Oncology-European Society of Gynaecological Oncology-European Society for Radiotherapy and Oncology) consensus conference together with biomolecular classification are currently applied to stratify patients into risk classes and in turn to assign the correct adjuvant treatment.

⇒ However, known prognostic factors cannot fully identify patients at risk of recurrence, especially in the early stages.

WHAT THIS STUDY ADDS

⇒ The proposed machine learning based model improves the prediction of the risk of recurrence of endometrial cancer by integrating well established risk class prognostic factors with new omic immunological features.

⇒ Furthermore, we found novel endometrial cancer immunological profiles that enabled ultrastratification of early stage cases, identifying those patients that experienced relapse despite being assigned to the low risk class.

HOW THIS STUDY MIGHT AFFECT RESEARCH, PRACTICE OR POLICY

⇒ In the endometrial cancer framework, our model can predict recurrence with a higher accuracy than guidelines parameters, opening up precision oncology approaches in terms of decision making, treatment, prognosis, and follow-up.

INTRODUCTION

Endometrial cancer is the sixth most common cancer in women and, although the mortality rate decreased in the past few decades, its incidence and prevalence rates are increasing worldwide.[1] Treatments for endometrial cancer are related to well known prognostic factors included in the risk classes defined by the ESMO-ESGO-ESTRO (European Society for Medical Oncology-European Society of Gynaecological Oncology-European Society for Radiotherapy and Oncology) consensus conference together with biomolecular classification.[2] However, these prognostic factors are not sufficient to predict the risk of recurrence of patients with early stage disease.

More recently, some studies have suggested the presence of an association between immunological signatures or specific tumor immune microenvironment subtypes and prognosis of women with endometrial cancer.[3 4] However, the integration of immune signatures

To cite: Bruno V, Betti M, D'Ambrosio L, *et al*. *Int J Gynecol Cancer* 2023;**33**:1708–1714.

to existing molecular based models has not been extensively evaluated, or mentioned in the guidelines.

Bioinformatics and machine learning tools are becoming important to address unsolved clinical questions in the current era of precision medicine. Recently, several methods to digitally deconvolve the tumor immune microenvironment and quantify immune populations within tissues have been developed to shed light on the immune context of different cancer types. Better characterization of the different risk classes in endometrial cancer is needed to improve patient clinical management and enable personalized therapy, with a major impact in terms of personalized medicine and surgical approach, even in women requiring fertility sparing techniques.

This study aims to investigate whether new omics derived predictive immune features, extracted from the Tumor Cancer Genome Atlas-Uterine Corpus Endometrial Carcinoma dataset (https://portal.gdc.cancer.gov/), can improve clinical risk prediction models. Furthermore, we also explored the potential and limitations of machine-learning approaches in this scenario.

METHODS

Dataset

The Tumor Cancer Genome Atlas-Uterine Corpus Endometrial Carcinoma dataset was downloaded from the Genomics Data Commons Data Portal (https://portal.gdc.cancer.gov/). Patients with endometrioid endometrial cancer and a non-null International Federation of Gynecology and Obstetrics (FIGO) stage (2009) annotation were selected; an additional filter on a 2 year minimum follow-up was applied to avoid short follow-up bias. The rationale behind the 2 year threshold resides both in the common agreement for the clinical practice and the observation that in the Tumor Cancer Genome Atlas-Uterine Corpus Endometrial Carcinoma dataset the distribution of relapse events within the third quantile falls within 25 months. A schematic representation of all of the steps in the dataset definition is provided in Figure 1A. The final dataset included 230 samples with a 1:3 ratio among the two groups (relapse and no relapse) with a median 42 month follow-up period (Figure 1B). Patients in the cohorts received different adjuvant treatments, ranging from no treatment to combined chemotherapy and radiotherapy (Figure 1C). Given the large time span in patients' year of diagnosis (1990–2016), the rationale behind treatment assignment was not fully defined and therefore treatment administration was not used as a predictive variable in the model but rather it was evaluated as a potential confounding factor.

To ensure the robustness and reproducibility of the tumor immune microenvironment population abundances estimation, three distinct deconvolution tools were used through the immunedeconv framework[5]: CIBERSORTx,[6] xCell[7] and quanTIseq.[8] These methods rely on a set of different algorithmic approaches and cell type signatures to estimate the relative abundance of different immune cell

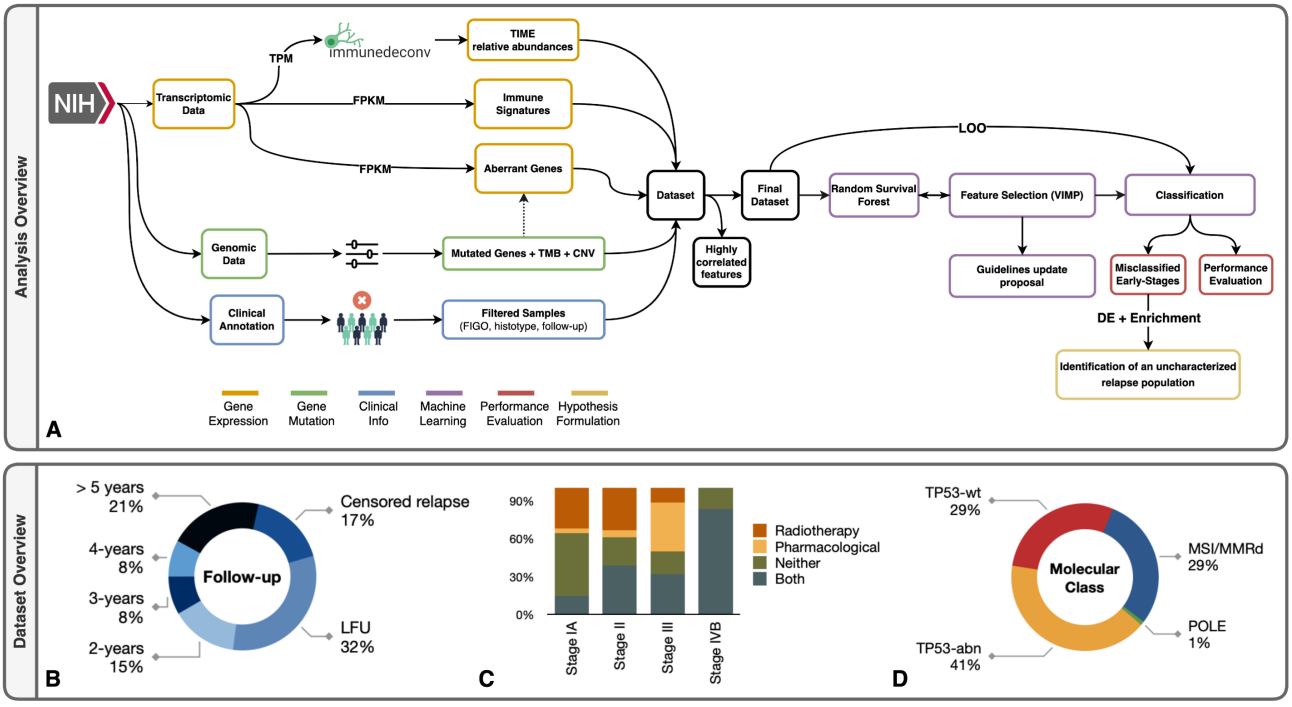

Figure 1 (A) Schematic workflow of dataset definition, model generation, and re-stratification proposal. (B) Overview of the Tumor Cancer Genome Atlas-Uterine Corpus Endometrial Carcinoma dataset (TCGA-UCEC) cohort follow-up. (C) Overview of the TCGA-UCEC cohort adjuvant treatment assignment by International Federation of Gynecology and Obstetrics (FIGO) stage. (D) Overview of the TCGA-UCEC cohort mutational profile. CNV, copy number variation; DE, differential expression; FPKM, reads per kilobase of exon per million reads mapped; LFU, lost in follow-up; LOO, leave-one-out; MSI, microsatellite instability; MMRd, mismatch repair deficiency; NIH, ; TIME, tumor immune microenvironment; TMB, tumor mutational burden; VIMP, variable importance predictor.

Table 1 Molecular markers

Feature	Definition
p53abn	TP53 deleterious mutation+CVN high
POLEmut	POLE deleterious mutation in exon 9–14+ tumor mutational burden high
CTNNB1mut	CTNNB1 deleterious mutation+low stage+TP53 mutated
L1CAMabn	L1CAM overexpression+TP53 wild type
Microsatellite instability	Deleterious mutation in one of ACVR2A, BTBD7, DIDO1, MRE11, RYR3, SEC31, SULF2
Tumor mutational burden	No of somatic mutations $\times 10^6$ over genome bases covered

populations by minimizing the distance between a specific cell expression profile and a subgroup of transcripts obtained through bulk RNA-Seq experiments. A consensus on population abundance was obtained by computing the median values per cell types, aggregated as described in online supplemental Table S1. Overall, a high level of agreement was found for the three methods (online supplemental Figure S1A), with greater variability per sample on most abundant populations, such as CD4+ T cells (online supplemental Figure S1B).

To better characterize the tumor immune microenvironment of samples, interferon γ, melanocytic plasticity signature, β-catenin, and transforming growth factor β signature scores were computed for each sample by calculating the geometric mean of expression levels of genes listed in online supplemental Table S2.[9–11] Regarding molecular features, the tumor mutational burden was calculated considering all non-synonymous variants that showed an allele frequency >5%, and the mutational status for TP53, POLE, and microsatellite instability features was defined according to the guidelines[12] described in Table 1 to produce molecular classes (Figure 1D) as in Kommos.[13] The PORTEC-4a clinical trial candidate biomarkers for risk class re-stratification such as the CTNNB1 feature,[9] and L1CAM high/low feature[14] based on the population median expression levels ("high" above the median, "low" below the median). Extremely unbalanced or highly correlated features (Pearson correlation >0.75) were excluded from the dataset to strengthen the interpretability of the model.

Statistical and Machine Learning Analysis

The RandomForestSRC[15] R package (V.3.1.0) was used to implement Breiman Random Forests regression, survival analysis, and class imbalanced q classification. The configuration was defined according to the numerosity, value ranges of variables, and target variable proportions. The baseline model was trained on a reduced set of features indicated in the guidelines and available in the Tumor Cancer Genome Atlas dataset (FIGO stage+p53 abn + POLEmut + mismatch repair deficiency/microsatellite instability) while for the immune integrated model, feature selection and model interpretability were performed using the internal variable importance predictor method. Disease free survival probability at each censoring time (Figure 2A) was predicted for each sample by performing an internal cross validation. Model performances were evaluated from confusion matrices through the balanced accuracy and precision metrics. The autoGO framework was used for differential gene expression analysis and multiple group comparisons.[16]

Gene correlation networks were generated from DEseq2[17] normalized counts, through a hard thresholding approach (Pearson correlation >0.75) while the differential network analysis was performed with a Gaussian modeling approach[18] (z score, t=4). The enrichment analysis was performed via autoGO,[19] testing all genes with a hub score >0.5. Statistical significance in differential expression analysis was adjusted for multiple comparisons (Bonferroni correction). Preprocessing steps were performed using Python (V. 3.9) and all statistical computations were performed in the R statistical environment (V. 4.1.2).

RESULTS

We describe the results related to the model, with particular emphasis on immune signatures exhibiting an impact on relapse prediction and overall prediction accuracy. We also provide a performance comparison of our model with the standard clinical and biomolecular guideline features in terms of recurrence prediction. Moreover, we describe three novel putative subtypes of stage IA–IB disease relying on their tumor related immunological profile.

Features Selection and Interpretation

We selected nine features according to the evaluation provided by the variable importance predictor (see methods) and assessed the marginal effect of each feature on disease free survival probability (Figure 2A). FIGO stage was the feature with the highest median value, along with a strong decrease in disease free survival probability for FIGO stage IIIB and a greater decrease for all classes of stage IV (Figure 2B, online supplemental Figure S2). However, while microsatellite instability and POLEmut status were strongly positively associated with better prognosis, pP53abn status did not exhibit a significant predictive power in our model.

Among selected immunological features, increasing levels of the relative abundance in tumor infiltrating immune cells of natural killer cells (up to 2.5%) and CD4+ T cells (up to 24.3%) were correlated with an increase in disease free survival probability (Figure 2A, online supplemental Figure S2). A stronger positive association with disease free survival probability was found for high tumor mutation burden values and for the interferon γ signature (median FPKM (reads per kilobase of exon per million reads mapped)), which also had an outstanding weight in the prediction (variable importance predictor coefficient >2, Figure 2B). In contrast, monocytes were correlated with a general decrease in disease free survival whenever their relative abundance was >0.6% (online supplemental Figure S2).

Model Performances

The baseline model trained on the set of features listed in the methods section reached a balanced accuracy of 53.7% and a true

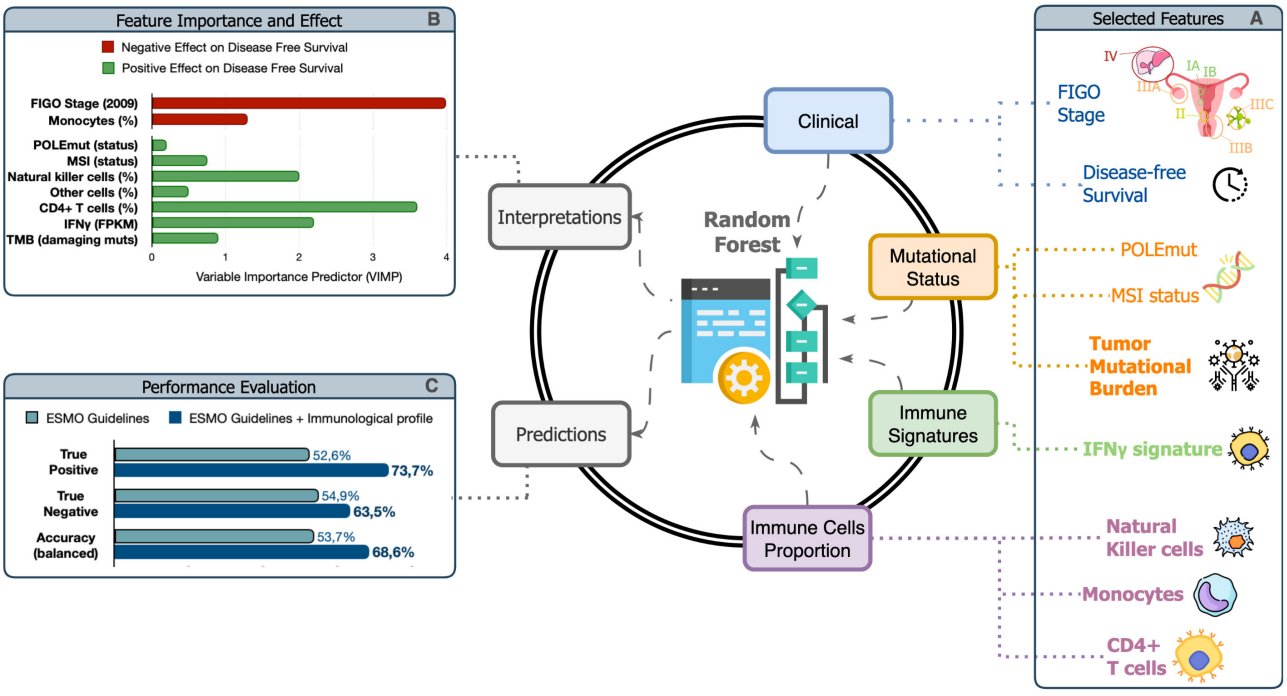

Figure 2 (A) Features selected for model training by variable importance predictor algorithm (novel features are in bold type). (B) Feature importance and effect on disease free survival. Higher values are associated with a stronger effect on predictions. Green bars are associated with a higher disease free survival probability; red bars are associated with a lower disease free survival probability. (C) Performances with and without novel features. True positives: percentage of correctly predicted high risk profiles. True negatives: percentage of misclassified high risk profiles. Accuracy: balance between true positives and true negatives. ESMO, European Society For Medical Oncology; FIGO, International Federation of Gynecology and Obstetrics; FPKM, reads per kilobase of exon per million reads mapped; IFN, interferon; MSI, microsatellite instability; TMB, tumor mutational burden.

positive rate of 52.6%, and was outperformed by our immune integrated model that reached 68.6% and 73.7% for balanced accuracy and true positive rate, respectively (Figure 2C). To evaluate the role of adjuvant treatment administration on our immune integrated model performance, we further assessed metrics specifically for FIGO stage and error type (Table 2) to highlight the incidence of patients that did not recur although exhibiting a high risk profile.

Re-stratification of Early Stages

Because a minority of early stage cases relapse regardless of their low risk profiles identified by our model, we sought to further investigate the factors that may help the re-stratification of these patients beyond our model. Thus we identified two groups of early stage patients: those that were predicted as low risk by the model but recurred (false negatives), defined as unexplained relapse early stages, and those that were correctly predicted as high risk patients (true positives), defined as characterized relapse early stages. We performed unexplained relapse early stages versus characterized relapse early stages and no relapse early stages multigroup gene expression comparison to highlight differences in relapse risk predictability.

According to the differential gene expression analysis, upregulated pathways in unexplained relapse early stages were mostly involved in chemokine/cytokine activity and antigen presenting activity, both in comparison with no relapse early stages and characterized relapse early stages (Figure 3A). Moreover, the differential expression network analysis showed that, in the unexplained relapse rarly stages co-expression network, an overall upregulation of genes involved in translation (Figure 3B) represented the main difference compared with both characterized relapse early stages and no relapse early stages. We further inspected tumor immune microenvironment deconvolution estimates to assess whether the results obtained from differential expression analysis could arise from the profiles of the immune cells rather than from the tumorous cells: we observed that the overall abundance of the tumor immune microenvironment represented, on average, 8% of the total amount of sequenced transcripts (Figure 3C). Moreover, the abundance was comparable among the three groups, suggesting that this aspect did not represent a relevant confounding factor for the differential expression analysis.

Table 2 Metrics by International Federation of Gynecology and Obstetrics (FIGO) stage

	Stage I	Stage II	Stage III	Stage IV
False positive rate (%)	25.6	27.2	35.8	22.2
False negative rate (%)	7.5	4.5	5.1	0
Correctly predicted (%)	66.8	68.2	59.1	77.8

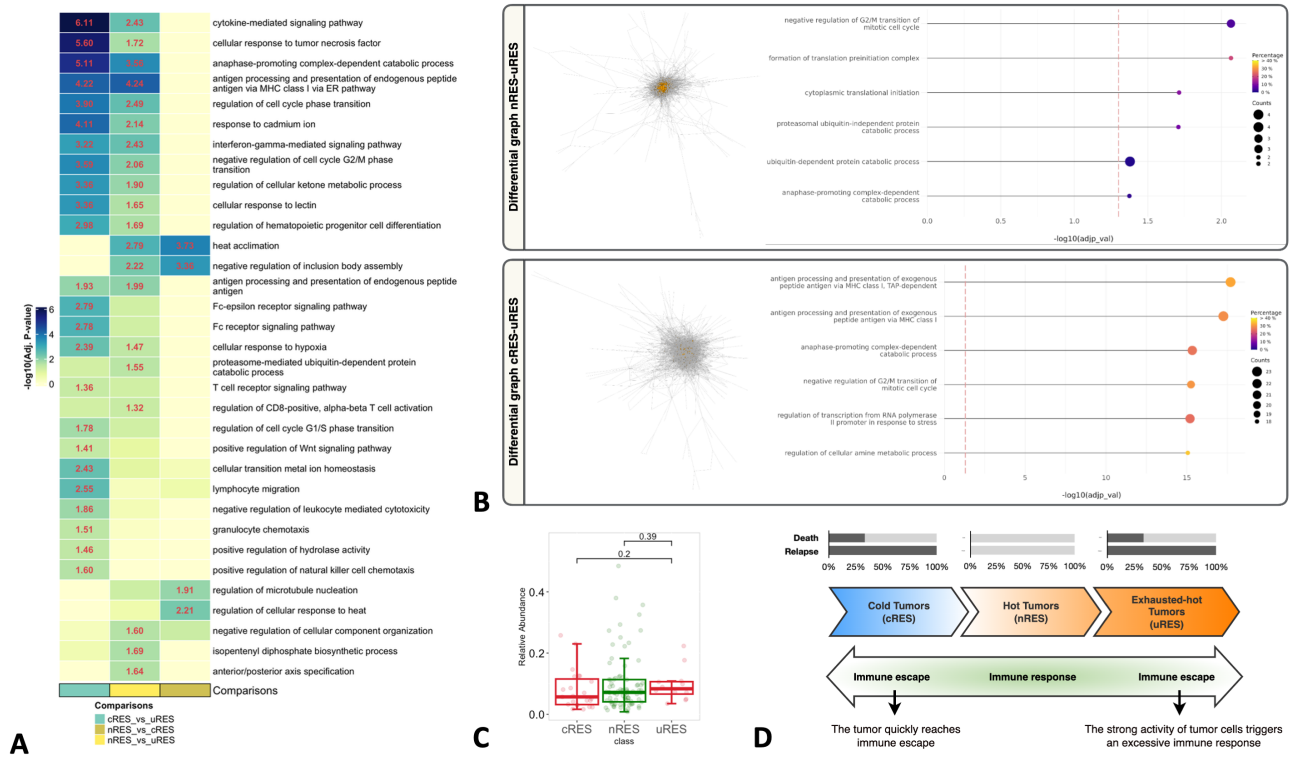

Figure 3 (A) Comparison heatmap of gene ontology (GO) biological processes terms enriched on upregulated genes in several differential expression analyses. Column annotations describe all of the comparisons between patient groups, with control versus condition notation. Red numbers indicate a significant difference in the expression of that pathway for a given comparison group. (B) Visual representation of unexplained relapse early stages (uRES) differential expression networks with respect to no relapse early stages (nRES) and characterized relapse early stages (cRES). Lolliplot: top six enriched biological pathways in genes with hub score >0.5 via autoGO; size and color of the dot represent, respectively, the absolute number and relative percentage of genes for a given enriched pathway. (C) Comparison of global tumor immune microenvironment abundances across uRES, cRES, and nRES. Boxplots shows the median value, interquartile range, and ±1.5 interquartile range. Wilcoxon test was used to assess significant differences in abundance distributions. (D) Summary of results and hypothesis on immune escape for exhausted hot profiles. Top annotation of relapse and death events (%) for each group.

DISCUSSION

Summary of Main Results

Our model resulted in an adequate choice for the proposed application due to its ability to deal with class imbalance, low numerosity, and feature interpretability. Moreover, the inclusion of immunological profiles, in addition to standard prognostic factors (see methods), increased the balanced accuracy of the model by 15%. Among mispredictions, most were false positive cases: one might suggest that, especially in stages II–IV, mispredictions are caused by the administration of adjuvant treatments which alter the natural course of the disease (Table 2).

Our results for the re-stratification analysis suggest that if no relapse early stages, characterized by an antitumor proinflammatory tumor immune microenvironment, could be considered as hot tumors, associated with a favorable prognosis, and characterized relapse early stages, characterized by a protumoral immune escaping tumor immune microenvironment, could be considered as cold tumors, associated with an unfavorable prognosis, then eventually, unexplained relapse early stages, characterized by an exhausted chronic proinflammatory tumor immune microenvironment, could be identified as exhausted hot tumors (Figure 3A), as reported in many studies.[20 21] We can therefore hypothesize that exhausted hot tumors may be a specific phenotype of early stage tumors for which tumor cells have a strong evolutive pressure to evade the potent innate immune response triggered by their proliferation and the release of inflammatory signals (Figure 3D).

Results in the Context of Published Literature

In the past decades, several attempts have been made to try to refine the classes of risk of endometrial cancer patients. Nevertheless, prognostic factors such as FIGO staging, grade, biomolecular classification, and ESMO-ESGO-ESTRO risk classes stratification fail in predicting patient outcomes, recurrence rate, and profile. In this regard, lack of evidence in the guidelines has been demonstrated.[3 22 23] Therefore, there is still a gap in the clinical management of endometrial cancer patients, because a better stratification could be closer to precision medicine.

In our study, the FIGO stage appeared to be the most significant feature; conversely, while relapse cases had a higher incidence in molecular high risk profiles (22% relapse in high, 17% relapse in medium, and 5% relapse in low), TP53 and POLE status did not have the expected impact on prediction.[24] Accordingly, guideline parameters alone reached a non-random balanced accuracy in recurrence prediction of 54%. Furthermore, L1CAM and CTNNB1, which have been associated in the literature with disease free survival and pattern of recurrence[14 25], did not appear to have a role

in outlining recurrence risk. These results, however, are not necessarily indicating the lack of association between the endpoint and the molecular markers; most likely this is due to the low informativity of mutational features for numerical reasons (feature imbalance and penalization of binary features).

Conversely, immunological markers, which are currently absent from the guidelines, were both a key factor for risk assessment in our model and identified uncharacterized high risk profiles in early stages. Among the most representative immune cells within the endometrium, the abundance of activated natural killer cells and CD4+ T cells, along with interferon γ signature level, could confer a minor risk to have recourse. These findings are in line with previous studies which showed that activated natural killer cells are associated with better overall survival, and enhanced CD8+ T cell activity is associated with higher disease free survival.[26] Furthermore, monocytes seem to be correlated with a general decrease in disease free survival, which is in line with our previous knowledge on macrophages M1/M2 balance role in prognosis.[22]

Strengths and Weaknesses

We engineered a workflow that can predict recurrence with higher accuracy than guideline parameters, by introducing the immune framework which has not yet been considered in endometrial cancer guidelines. We also found that among misclassified patients, novel and uncommon immune profiles could provide further stratification in the early stage population.

Some limitations have been found in the methodology: class imbalance and numerosity represent the greatest limitations of this study, along with the heterogeneity of clinical data due to the multicentre nature of the dataset. Moreover, false positive cases are, predictably, the main source of error for two independent reasons: (i) administration of adjuvant treatments inevitably produces many spurious over treatment cases, proportionally to the efficacy of the treatment; and (ii) from a more technical point of view, the model is designed to optimize both true positive and true negative rates to facilitate the correct classification of the minority class (relapse), which inevitably introduces bias.

Implications for Practice and Future Research

We propose an integrated clinical, molecular, and immune related model which paves the way for further validation in clinical practice. Our results suggests that the next step in endometrial cancer management would be to identify all of the different endometrial cancer profiles, which in turn would have different patterns of recurrence: through this step, we could approach precision oncology and tailored surgery, to be able to address potential fertility sparing treatment in young patients, a tuned surgical approach, and a proper follow-up schedule in a postoperative setting, according to every profile and pattern of recurrence.[27] Potential developments of our work foresee the validation of the model on other cohorts and the testing on other data sources, such as hematoxylin and eosin scans and molecular diagnostics, which are more suitable for application in the clinical context. Finally, our results in the early stages could be further explored to identify putative immunotherapy biomarkers.

CONCLUSIONS

We have introduced a machine learning based model to improve prediction of the risk of recurrence of endometrial cancer, by integrating well established risk class prognostic factors with new omics derived immunological features so far neglected by the guidelines. Furthermore, we found novel endometrial cancer immunological profiles that enabled ultrastratification of early stage cases, identifying those patients that relapsed despite being assigned to the low risk class. In the endometrial cancer framework, our model can predict recurrence with a higher accuracy than guideline parameters, opening up precision oncology approaches in terms of decision making, treatment, prognosis, and follow-up.

Author affiliations
[1]Department of Experimental Clinical Oncology, IRCCS Regina Elena National Cancer Institute, Rome, Italy
[2]Alleanza Contro il Cancro, Rome, Italy
[3]IRCCS Regina Elena National Cancer Institute, Rome, Italy
[4]Section of Ginecology and Obstetrics, Department of Surgical Sciences, University of Rome Tor Vergata, Roma, Italy
[5]Division of Gynecologic Oncology, Michele and Pietro Ferrero Hospital, Verduno, Italy

Contributors Conceptualization: VB, MB, MP, and EV. Data curation: VB, MB, and LDA. Formal analysis: MB and LDA. Funding acquisition: VB, GC, and MP. Investigation: VB, MB, LDA, AM, GP, PN, MP, and EV. Methodology: MB, LDA, AM, and AB. Project administration: VB and GC. Resources: GC and EV. Software: MB, LDA, and AM. Supervision, validation, and visualization: VB, PN, and MP. Roles/writing-original draft, VB, MB, LDA, and MP. Writing-review and editing, VB, MB, LDA, AM, BC, AP, AB, GP, GC, PN, MP, and EV. Guarantor: VB.

Funding This work was supported by the Italian Ministry of Health (Ricerca Corrente). We acknowledge Alleanza Contro il Cancro (ACC) for MB's fellowship under the GERSOM project.

Competing interests None declared.

Patient consent for publication Not applicable.

Ethics approval Not applicable.

Provenance and peer review Not commissioned; externally peer reviewed.

Data availability statement Data are available in a public, open access repository. All data relevant to the study are included in the article or uploaded as supplementary information. Data availability https://portal.gdc.cancer.gov.

ORCID iDs
Martina Betti http://orcid.org/0009-0003-4462-2207
Lorenzo D'Ambrosio http://orcid.org/0000-0002-9656-7436
Alessandro Buda http://orcid.org/0000-0002-7093-6862

REFERENCES

1 Siegel RL, Miller KD, Jemal A. Cancer statistics, 2020. *CA Cancer J Clin* 2020;70:7–30.
2 Colombo N, Creutzberg C, Amant F, *et al*. ESMO-ESGO-ESTRO consensus conference on endometrial cancer: diagnosis, treatment and follow-up. *Ann Oncol* 2016;27:16–41.
3 Li BL, Wan XP. Prognostic significance of immune landscape in tumour microenvironment of endometrial cancer. *J Cell Mol Med* 2020;24:7767–77.
4 Ding H, Fan G-L, Yi Y-X, *et al*. Prognostic implications of immune-related genes' (Irgs) signature models in cervical cancer and endometrial cancer. *Front Genet* 2020;11:725.
5 Sturm G, Finotello F, Petitprez F, *et al*. Comprehensive evaluation of transcriptome-based cell-type quantification methods for immuno-oncology. *Bioinformatics* 2019;35:i436–45.
6 Newman AM, Steen CB, Liu CL, *et al*. Determining cell type abundance and expression from bulk tissues with digital cytometry. *Nat Biotechnol* 2019;37:773–82.
7 Aran D, Hu Z, Butte AJ. xCell: digitally portraying the tissue cellular heterogeneity landscape. *Genome Biol* 2017;18:220.
8 Plattner C, Finotello F, Rieder D. Deconvoluting tumor-infiltrating immune cells from RNA-Seq data using quanTIseq. *Methods Enzymol* 2020;636:261–85.
9 Ayers M, Lunceford J, Nebozhyn M, *et al*. IFN-Γ-related mRNA profile predicts clinical response to PD-1 blockade. *J Clin Invest* 2017;127:2930–40.
10 Pérez-Guijarro E, Yang HH, Araya RE, *et al*. Multimodel preclinical platform predicts clinical response of melanoma to immunotherapy. *Nat Med* 2020;26:781–91.
11 Mariathasan S, Turley SJ, Nickles D, *et al*. TGFβ attenuates tumour response to PD-L1 blockade by contributing to exclusion of T cells. *Nature* 2018;554:544–8.
12 Nicoletta CC, Amant F, Bosse T, *et al*. ESMO-ESGO-ESTRO consensus conference on endometrial cancer - endometrial cancer pocket guidelines. *Int J Gynecol Cancer* 2017;26.
13 Kommoss S, McConechy MK, Kommoss F, *et al*. Final validation of the promise molecular classifier for endometrial carcinoma in a large population-based case series. *Ann Oncol* 2018;29:1180–8.
14 Kommoss FK, Karnezis AN, Kommoss F, *et al*. L1CAM further stratifies endometrial carcinoma patients with no specific molecular risk profile. *Br J Cancer* 2018;119:480–6.
15 Kogalur U, Ishwaran H. randomForestSRC: fast unified random forests for survival, regression, and classification (RF-SRC). *R Package Version* 2019;2. Available: https://www.randomforestsrc.org/articles/getstarted.html
16 Sperandio E, Grassucci I, D'Ambrosio L, *et al*. Automated, reproducible investigation of gene set differential enrichment via the AUTO-go framework. *Bioinformatics* [Preprint] 2022.
17 Love MI, Huber W, Anders S. Moderated estimation of fold change and dispersion for RNA-Seq data with Deseq2. *Genome Biol* 2014;15:550.
18 He H, Cao S, Zhang J, *et al*. A statistical test for differential network analysis based on inference of Gaussian graphical model. *Sci Rep* 2019;9.
19 Chen EY, Tan CM, Kou Y, *et al*. Enrichr: interactive and collaborative HTML5 gene list enrichment analysis tool. *BMC Bioinformatics* 2013;14:128.
20 Zhang Z, Liu S, Zhang B, *et al*. T cell dysfunction and exhaustion in cancer. *Front Cell Dev Biol* 2020;8.
21 Guo Y-E, Li Y, Cai B, *et al*. Phenotyping of immune and endometrial epithelial cells in endometrial carcinomas revealed by single-cell RNA sequencing. *Aging (Albany NY)* 2021;13:6565–91.
22 Vanderstraeten A, Tuyaerts S, Amant F. The immune system in the normal endometrium and implications for endometrial cancer development. *J Reprod Immunol* 2015;109:7–16.
23 Liu W, Sun L, Zhang J, *et al*. The landscape and prognostic value of immune characteristics in uterine corpus endometrial cancer. *Biosci Rep* 2021;41:BSR20202321.
24 Stelloo E, Nout RA, Osse EM, *et al*. Improved risk assessment by integrating molecular and clinicopathological factors in early-stage endometrial cancer-combined analysis of the PORTEC cohorts. *Clin Cancer Res* 2016;22:4215–24.
25 Imboden S, Tapia C, Scheiwiller N, *et al*. Early-stage endometrial cancer, CTNNB1 mutations, and the relation between lymphovascular space invasion and recurrence. *Acta Obstet Gynecol Scand* 2020;99:196–203.
26 Bruno V, Corrado G, Baci D, *et al*. Endometrial cancer immune escape mechanisms: let us learn from the fetal–maternal interface. *Front Oncol* 2020;10.
27 Tanos P, Dimitriou S, Gullo G, *et al*. Biomolecular and genetic prognostic factors that can facilitate fertility-sparing treatment (FST) decision making in early stage endometrial cancer (ES-EC): a systematic review. *Int J Mol Sci* 2022;23:2653.

Supplementary

Figure S1: (A) Marginal variable effect on disease-free survival probability. The variable status "0" indicates the absence of the parameters required to define the feature. For continuous variables, the values indicated on the x-axis have been normalized and do not indicate the actual feature value. The y-axis indicated the disease-free survival probability. The x-axis rug represents the number of samples that represent the interval, therefore the robustness of the variable marginal effect for a given range of values. Ranges above the starting value (*y* value at *x=0*) are associated to a positive prognostic effect for that given feature. **(B)** Variable importance predictor coefficient for each selected feature. Higher median values are associated to a higher average impact on predictions.

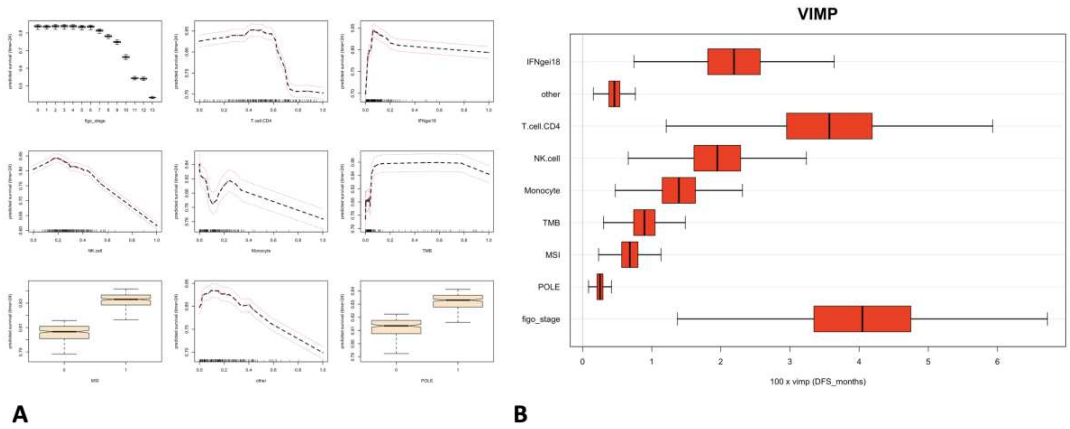

Figure S2: Comparison of cell abundances distributions in multiple in-silico deconvolution tools for shared cell populations.

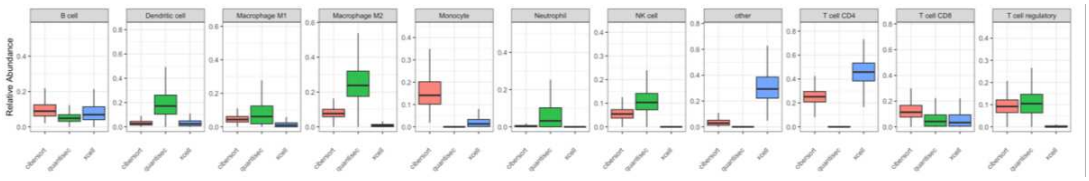

Figure S3: (A) Gene correlation network characterized relapse early stages with node size equals to 1% of the node degree. **(B)** Gene correlation network no-relapse early stages with node size equals to 1% of the node degree. **(C)** Gene correlation network unexplained relapse early stages with node size equals to 1% of the node degree.

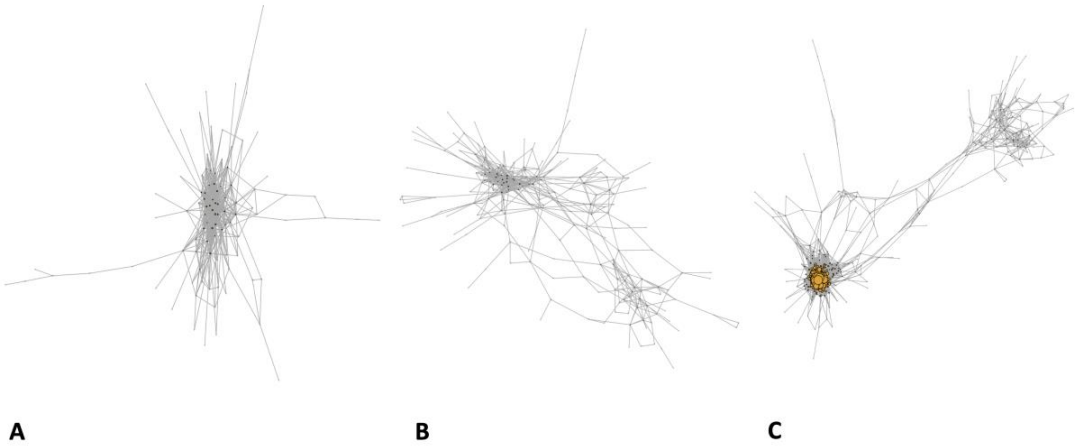

Table S1: In-silico deconvolution tools aggregation schema. Immune cells sub-types have been aggregated to allow for comparison.

quanTIsec	CIBERSORTx	xCell	Variation
T cells CD4+	T cells CD4 naive, T cells CD4 memory resting, T cells CD4 memory activated, T cells follicular helper	T cell CD4+ Th1, T cell CD4+ Th2, T cell CD4+ naive, T cell CD4+ memory, T cell CD4+ central memory, T cell CD4+ effector memory	8.9 %
T cells CD8+	T cells CD8	T cell CD8+ effector memory, T cell CD8+ central memory, T cell CD8+ naive	0.5%
Natural killer cells	NK cells resting, NK cells activated	NK cells	0.1%
Tregs	T cells regulatory	T cell regulatory	0.03%
Neutrophils	Neutrophils	Neutrophils	0.003 %
Dendritic cells	Dendritic cells resting, Dendritic cells activated	Myeloid dendritic cell, Plasmacytoid dendritic cell	0.07 %
Monocytes	Monocytes, Macrophages M0	Macrophages, Monocytes, Granulocyte-monocyte progenitor	0.8%
Macrophage M1	Macrophages M1	Macrophages M1	0.06%
Macrophage M2	Macrophages M2	Macrophages M2	0.02%
B cells	B cells naive, B cells memory, Plasma cells	B cell plasma, Class-switched memory B cell, B cell memory, B cell naive	0.4 %
-	T cells gamma delta, Mast cells resting, Eosinophils	T cell NK, Common lymphoid progenitor, Common myeloid progenitor, Eosinophil, Granulocyte-monocyte progenitor, Hematopoietic stem cell, Mast cell	3.8%

Table S2: Immune signature genes.

Name	Genes

IFNγ extended	CD3D,IL2RG,NKG7,CIITA,HLA-E,CD3E,CXCR6,CCL5,LAG3,TAGAP,GZMK,CD2, IDO1,CXCL10,HLA-DRA,STAT1,CXCL13,GZMB
TGFβ	ACTA2, ACTG2, ADAM12, ADAM19, CNN1, COL4A1, CTGF, CTPS1, FAM101B, FSTL3, HSPB1, IGFBP3, PXDC1, SEMA7A, SH3PXD2A, TAGLN, TGFBI, TNS1, TPM1
MPS	AKR1C3, BMP1, CRTAC1, ECEL1, ERC2, FAM110C, FUT9, GABRA2, GAP43, GREM1, HECW1, KLHL1, KRT12, LHFPL4, NEFL, NEFM, NETO1, NKX2-2, NSG2, OCIAD2, OTOP1, PDE3B, PTPRN2, PTPRT, SIGLEC15, SLC13A5, SLC9A2, SLITRK6, SNAP91, STON2, TAC1, VAT1L, WNT5A, ALX1, BRD7, DTD1, GRSF1, HCN1, LTA4H, OXCT1, PATJ, PLXNC1, SSBP4, TELO2, TMEM177
βCatenin	AKR1C3,BMP1,CRTAC1, ECEL1, ERC2, FAM110C, FUT9, GABRA2, GAP43, GREM1, HECW1, KLHL1, KRT12, LHFPL4, NEFL, NEFM, NETO1, NKX2-2, NSG2, OCIAD2, OTOP1, PDE3B, PTPRN2, PTPRT, SIGLEC15, SLC13A5, SLC9A2, SLITRK6, SNAP91, STON2, TAC1, VAT1L, WNT5A, ALX1, BRD7, DTD1, GRSF1, HCN1, LTA4H, OXCT1, PATJ, PLXNC1, SSBP4, TELO2, TMEM177